MINERALOGICAL MAGAZINE

VOLUME 60 NUMBER 401 AUGUST 1996

The conditions of metamorphism of a grossular–wollastonite vesuvianite skarn from the Omey Granite, Connemara, western Ireland, with special reference to the chemistry of vesuvianite

Y. AHMED-SAID* AND BERNARD E. LEAKE

Department of Geology and Applied Geology, University of Glasgow, Glasgow G12 8QQ, UK

Abstract

The Fountain Hill skarn, which was produced by thermal metamorphism of impure limestone in the Omey Granite aureole, consists of wollastonite, calcite, grossular-andradite garnet, diopside, B-free vesuvianite and small amounts of albite, K-feldspar and quartz. Zoning in vesuvianite is, overall, independent of birefringence but oscillatory concentric zoning in the mineral is controlled mainly by Ti. In addition to extensive within-site substitutions (e.g. F for OH in the OH-sites, Fe^{2+} for Mg, Fe^{3+} for Al, Ti for Al etc. in the Y-sites), there are significant cross-site combined substitutions involving Y–X and Y–Z but not X–Z sites so that ideal solution models for this mineral are not applicable. The thermodynamic mole fraction of Hoisch (1985) is modified to account for the excess of the ΣY cations in the Y sites and can be applied to both B-bearing and B-free vesuvianites. Using the thermodynamic dataset of Holland and Powell (1990) and taking into account the existence of andalusite, sillimanite and corundum in associated pelites, leads to the conclusion that the metamorphic conditions were about 640 ± 20°C and 3.3 ± 0.3 kb at 0.15 ± 0.05 X_{CO_2}.

KEYWORDS: activity, grossular, hornfels, thermodynamic mole fraction, vesuvianite, wollastonite.

Introduction

THE circular 6.5 km diameter Omey Granite in western Connemara, Co. Galway, Ireland, which was described by Townend (1966) and dated at about 415 Ma by Leggo *et al.* (1966), intrudes the Dalradian Connemara schists with development of a metamorphic aureole. The earlier regional metamorphisms in the Dalradian rocks to the SE of the granite produced quartz-plagioclase-biotite-muscovite-garnet-staurolite with rare kyanite followed by fibrolite sillimanite in the pelites. The Omey aureole developed andalusite, cordierite, new biotite, and microcline in pelites up to 1400 m from the granite with prismatic sillimanite and corundum in the inner aureole (< 250 m from the contact) and in marbles garnet-wollastonite-calcite up to 470 m from the granite (Ferguson and Harvey, 1979; Ferguson

---

* Previous address: Oum-Toub (Skikda), P.O. Box 56, 21450, Algeria

Mineralogical Magazine, August 1996, Vol. 60, pp. 541–550

TABLE 1. Mineral chemistry

	Garnet		Diopside		Plagioclase		Wollastonite			Vesuvianite	
Oxides	maximum		$\bar{x}$	σ	$\bar{x}$	s					
	rim	core									
SiO_2	38.55	39.56	52.59	0.28	67.39	0.65	51.41	0.23		35.83	35.65
TiO_2	0.76	0.15	0.06	0.01			0.04	0.016		2.76	0.46
Al_2O_3	16.30	19.75	0.70	0.18	20.73	0.56	0.06	0.06		16.92	18.97
Fe_2O_3	8.59	3.81	1.15	0.07			0.28	0.08		1.72	1.51
FeO	1.70	0.41	6.27	0.39	T					2.02	1.77
MgO	0.05	0.01	13.23	0.34						1.89	1.83
MnO	0.30	0.24	0.48	0.32			0.13	0.05		0.06	0.02
CaO	34.88	36.50	24.83	0.04	0.07	0.02	45.5	0.26		36.15	35.12
Na_2O			0.17	0.03	10.84	0.78				0.16	0.09
K_2O				0	0.06	0.02			F	1.56	2.06
Total	101.13	100.47	99.48		99.09		97.42			99.53	97.83
Cations on 24 oxygens for garnet, 6 for diopside, 32 for feldspars, and 18 for wollastonite and 50 cations for vesuvianite											
Si	5.934	6.001	1.973	0.004	11.846	0.132	5.999	0.013		17.438	17.536
Al^{IV}	0.066	–	0.027	0.005	4.295	0.105	0.014	0.013		0.562	0.440
Al^{VI}	2.842	3.530								9.143	10.57
Ti	0.088	0.170	0.0012	0.0002			0.003	0.001		1.010	0.170
Fe^{3+}	0.996	0.434	0.033	0.005			0.025	0.007		0.630	0.560
Fe^{2+}	0.218	0.052	0.197	0.015						0.822	0.729
Mg	0.012	0.002	0.740	0.021						1.371	1.344
Mn	0.040	0.03	0.015	0.010			0.013	0.005		0.025	0.008
Ca	5.758	5.936	0.998	0.004	0.013	0.004	5.940	0.009		18.848	18.532
Na			0.012	0.002	3.691	0.252		0.0012		0.150	0.086
K					0.011	0.005					
									F^-	2.40	3.20
									O^{2-}	1.0	1.0
									OH^-	6.60	5.62

The minerals were analysed in the Department of Geology and Applied Geology, University of Glasgow using a Camebax SX 50 microprobe. All analyses were performed with an accelerating voltage of 15 kv (30 kv for trace elements), sample current of 5 μA, counting time of 10–30 s using a beam of 5 μm in diameter. ZAF corrections were applied to all apparent concentrations. $\bar{x}$ is the average of four minerals with four analysed spots per mineral, Fe^{2+} and Fe^{3+} are calculated on charge balance basis except for vesuvianites where $Fe^{2+} = 0.54Fe^{3+}$ (see text for more details), T = trace. Vesuvianites contain B 0.00, 0.00; SO_2 0.01, 0.13; ZnO 0.00, 0.00; Cl 0.00, 0.02.

and Al-Ameen, 1985). The hornfelsing of the pelites has been studied in some detail by the latter authors who deduced conditions of 615 ± 25°C at 2.5 ± 0.25 kbar and with localized flow of an H_2O-rich fluid away from the granite but the skarns and their minerals have not been previously described in detail. New understanding of the role of boron in vesuvianite (Groat *et al.*, 1992*a*) also makes the study of assemblages including this mineral more profitable than previously.

The skarns occur where marble in the Lakes Marble Formation (Leake and Tanner, 1994) is within 300 m from the granite margin and especially good exposures occur at Fountain Hill beach on the south side of the Omey Granite about 140–150 m south of the granite contact. The marble bands in the Lakes Marble Formation are generally calcite marbles following the regional metamorphism of the Dalradian rocks as distinct from the green ophicalcitic 'Connemara Marble' used ornamentally, which represents a metamorphosed siliceous dolostone and has been described in detail by Leake *et al.* (1975). The Lakes Marbles regionally contain quartz, phlogopite, titanite, diopside and K-feldspar with voluminous calcite and were presumably derived from original sedimentary quartz, clay minerals (especially illite) and Mg-bearing calcite in a limestone and the "impurities" reacted with calcite to give the skarn silicates during partial decarbonation of the calcite.

Mineralogy

Near the contact, the rocks consist of wollastonite, calcite, diopside, garnet, vesuvianite, and small amounts of albite and K-feldspar with accessory zircon. Garnet occurs as both poikiloblastic grains (usually 5–10 mm in diameter but up to 30 mm) containing calcite, diopside, wollastonite and quartz inclusions or less commonly as inclusion-free euhedral crystals 5 mm in diameter. Like garnet, vesuvianite, which is brown in hand specimen and colourless to slightly pinkish in thin section, is also found as euhedral and anhedral grains; the latter are most common and usually replace calcite and garnet, and these two minerals together with wollastonite and diopside are also found as inclusions within the vesuvianite. The euhedral vesuvianites, 6 mm in diameter, are inclusion-free and replaced plagioclase. Diopside (<1 mm) occurs as isolated grains or as inclusions in anhedral garnet and vesuvianite. Wollastonite, which sometimes replaced garnet, vesuvianite, diopside and calcite, is found as radial aggregates with big elongated crystals displaying simple twinning. Albite is scarce but calcite is ubiquitous. Chemical analyses of the minerals are given in Table 1.

Both garnet types exhibit the same zoning pattern, having Ti- and Fe-rich cores without significant variations of Mn, Mg and Ca. The maximum core and rim compositions are $Gross_{87.30}And_{11.68}Sp_{0.50}Alm_{0.49}Pyr_{0.03}$ and $Gross_{68.20}And_{28.55}Alm_{2.41}Sp_{0.66}Pyr_{0.18}$ respectively. Plagioclase is unzoned albite containing variable amounts of Sr (0–2198 ppm) with only little Ba (Ba = 0–300 ppm). Wollastonite is also unzoned, does not form solid solutions with pyroxene, and is an almost pure calcium silicate with only small substitutions of Fe and Mn for Ca. Sr is detected in all analysed wollastonites and averages 761±307 ppm (range 507–1353 ppm). Diopside is uniform $Ca_{49.90}Fe_{13.1}Mg_{37.00}$ with 676 ppm Sr and 0.11 wt.% ZnO.

Recent structural refinements of vesuvianite (Hoisch, 1985; Valley *et al.*, 1985; Groat *et al.*, 1992*a*,*b*, 1994*a*,*b* , 1995) suggest that the formula has the basis of 50 cations. This normalization scheme agrees well with the number of available sites in the ideal structure of B-free vesuvianites based on the formula $X_{19}Y_{13}Z_{18}O_{68}W_{10}$ where X = Ca, Na, *REE*, Pb^{2+}, Sb^{3+}; Y = Al, Mg, Fe^{3+}, Fe^{2+}, Ti^{4+}, Mn, Cu, Zn; Z = Si and W = OH, F, O. However, Groat *et al.* (1994*a*) noted that a few B-free vesuvianites have a Y-group total (ΣY) significantly higher than the ideal value of 13 and hence they recalculated the mineral formula on the basis of 18 Si instead. Four of this "small number of exceptional vesuvianite crystals" were further refined by these authors and their results showed the Z-sites to be exclusively occupied by Si which lead them to suggest an additional tetrahedrally coordinated site ($T1$). In B-free vesuvianites, these $T(1)$ sites are either vacant or partly occupied by the excess (Al, Fe^{3+}) which lead to a new revised formula $X_{19}Y_{13}T(1)_5Z_{18}O_{68}W_{10}$ where $T(1)$ = Al, Fe^{3+} in excess of the 13 cations in the Y sites (see below).

We have renormalized the four "exceptional vesuvianites" studied by Groat *et al.* (1994*a*) on the basis of 50 cations and plotted them with many B-free vesuvianites in Fig. 1. There are a number of interesting features: (1) the four "exceptional vesuvianites" have Si = 17.92±0.13 a.p.f.u. (atoms per formula unit) which is statistically the same to the ideal value of 18 a.p.f.u. The same applies to the vesuvianites of Hoisch (1985) and Groat *et al.* (1992*a*, 1994*a*, 1995). (2) There is no correlation between Al and Si (R = 0.00) for vesuvianites published by these authors either as separate groups or all together, thus excluding any Al for Si substitutions. (3) ΣY-cations>13 a.p.f.u. for all vesuvianites shown in Fig. 1 except four samples published by Groat *et al.* (1995).

The Connemara vesuvianites are strikingly different; they are generally more aluminous

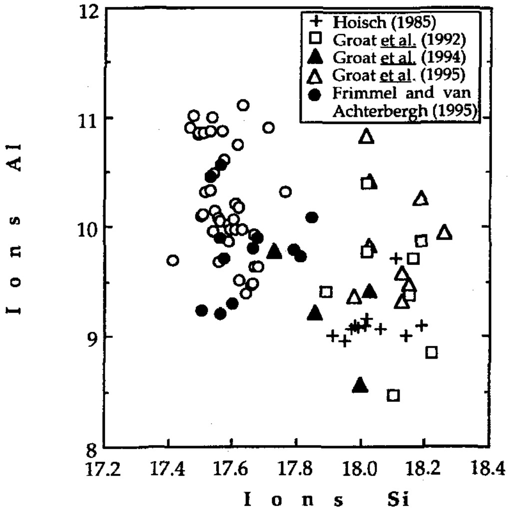

FIG. 1. Al *vs.* Si showing Al for Si substitution in the Connemara vesuvianites (open circles). Note also the broad negative correlation between the two ions for the analyses as a whole.

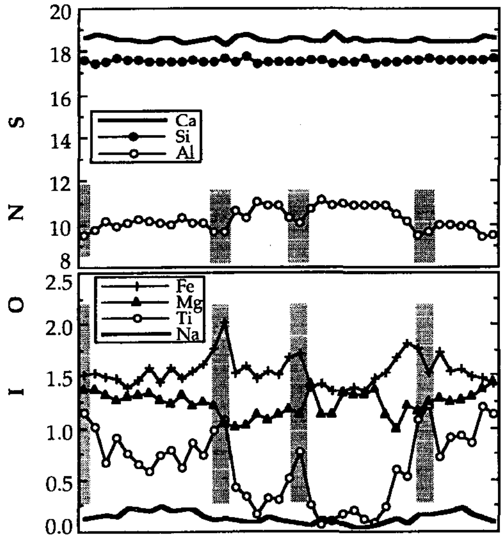

FIG. 2. A traverse through a 2.5 mm zoned vesuvianite (ions based on 50 cations). Stipple areas are exaggerated high-birefringence zones.

(Al = 10.24±0.50 a.p.f.u.), less siliceous (Si = 17.58±0.07 a.p.f.u.) and more importantly, Al and Si correlate antipathetically, suggesting continuous Al for Si substitutions. Particularly relevant is that, with the exception of the four vesuvianites mentioned above, all vesuvianites shown in Fig. 1 have ΣY cations in excess of 13 which make it a common rather than an exceptional feature. The Connemara vesuvianites were checked for accuracy and the existence of Si-deficient vesuvianites from other localities (Fig. 1) supports the fact that our data are not exceptional.

Some of the Connemara vesuvianites display oscillatory concentric birefringence-zoning with alternating low and high birefringence zones. There is a general decrease in Al and Fe and increase in Ti and Mg from core to rim in the low birefringence zones (Fig. 2) or in the optically unzoned grains. The high birefringence zones are very narrow and systematically characterized by low Al and high Ti contents (Fig. 2). Although Fe tends to be higher and Mg lower in the high birefringence zones, the trends are not always maintained especially toward the rims (Fig. 2). Aluminium can also be eliminated because zones of high and low birefringence can have similar Al concentrations (compare high birefringence zones in the rims with low birefringence zones in the cores in Fig. 2). It is therefore concluded that the high birefringence zones are related to high Ti concentrations in agreement with previous findings (e.g. Kerrick *et al.*, 1973; Gibson and Wallmach, 1995). Traverses through the mineral allowed direct substitutional studies (Fig. 2; Table 2*a*; see also Table 2*b* for a summary of statistics of the analysed mineral). Table 2*a* shows very important facts:

(1) ΣX- and ΣZ-cations do not correlate (R=0.05) excluding any interactions among the cations occupying these sites

(2) ΣY- and ΣZ-cations exhibit a negative correlation (R = −0.13) which is principally due to Al and to a lesser extent Ti substitutions for Si (R = −0.11 and −0.09 respectively).

(3) ΣY- and ΣX-cations display a strong antipathetic correlation (R=−0.67) indicating strong interactions among the various X and Y sites, probably through combined substitutions.

It is, however, relevant to establish substitutions in each site first. Thus, Table 2*a* shows that there is no significant one to one Na substitution for Ca (R=−0.05) *within the X sites* but combined substitutions involving the unanalysed *REE*, which preferably occupy the *X* sites, are possible (Groat *et al.*, 1992*a*,*b*). There are a large number of substitutional possibilities among the Y cations but these are dominated by Ti for Al replacements. These include: $Fe^{2+} = Mg^{2+}$; $Fe^{3+} = Al^{3+}$; $Fe^{2+} + Ti^{4+} = 2Al^{3+}$; $Mg^{2+} + Ti^{4+} = 2Al^{3+}$ and possibly (Groat *et al.*, 1992); $H^{+} + Al^{3+} = Ti^{4+}$; $Mg^{2+} + OH^{-} = Al^{3+} + O^{2-}$; $Fe^{2+} + OH^{-} = Al^{3+} + O^{2-}$; $Ti^{4+} + O^{2-} = Al^{3+} + OH^{-}$. Substitutions involving Mn are less clear due to its low concentrations in the mineral (Mn = 0.02±0.01 a.p.f.u.) but positive correlation between Mn and Mg suggests that both elements follow similar trends rather than substitute for one another. In the Z sites: $Ti^{4+} = Si^{4+}$ and $Al^{3+} + H^{+} = Si^{4+}$. Many possibilities exist for $X - Y$ cation group substitutions (Table 2) but only those which are believed realistic are given: $Na^{+}\ Ti^{4+} = Ca^{2+} + Al^{3+}$; $Na^{+}\ Ti^{4+} = Mg^{2+} + Al^{3+}$; $Ca^{2+} + Mg^{2+} = Na^{+} + Al^{3+}$; $Ca^{2+} + Mg^{2+} = 2Fe^{2+}$; $Na^{+} + Al^{3+} = Ti^{4+}$; $Na^{+} + Al^{3+} = 2Fe^{2+}$; $Na^{+} + Al^{3+} = Fe^{2+} + Ca^{2+}$; $Ca^{2+} + Na^{+} = Al^{3+}$; $Ca^{2+} + Mg^{2+} = Fe^{3+}$+ Na+. It should be emphasized that the strong negative correlations in the equations involving Ti and Al on each side are strongly governed by Ti for Al substitution.

There is a decrease of the ΣY cations in passing from the vesuvianite core to rim which can be reliably attributed mainly to Al and to a lesser extent Fe (Figs 2 and 3) implying that the excess of the Y cations over 13 a.p.f.u. is related to these cations. Groat *et al.* (1994*a*) showed that the Y group excesses, which they also attributed to Al and Fe in B-free vesuvianites, occupy a T(1) site which is a tetrahedrally coordinated site linked to anions occupying O(7) and O(11). Based on local bond valence of their studied vesuvianites, these authors suggested two main substitutions:

$$^{T(1)}(\mathrm{Al,Fe}) + {}^{H(1)}\diamond 4 = {}^{T(1)}\diamond 2 + {}^{H(1)}\mathrm{H}4 + {}^{X(3)}\mathrm{Ca}$$

TABLE 2. (A) inter-cationic correlations showing possible ionic substitutions in Connemara vesuvianites (negative correlations are indicated by a minus sign), and (B) summary statistics of 39 vesuvianite analyses

A

Si	Ti	Al	Fe	Mn	Mg	Ca	Na	Na+Ti	Ca+Al	Mg+Ti	Na+Al	Ca+Mg	Al+Mg	Σ*X*	Σ*Y*	Σ*Z*(Si)	19-Σ*X*	
1	−0.09	−0.11	0.01	0.00	0.00	0.06	0.00	0.07	−0.15	0.07	0.12	−0.02	−0.12	0.05	−0.13	1	0.06	Si
	1	−0.94	+0.16	+0.05	+0.05	0.00	0.25	0.98	−0.94	0.92	−0.92	0.03	−0.92	0.06	−0.17	−0.09	−0.06	Ti
		1	−0.18	−0.05	−0.08	0.01	−0.20	−0.92	0.95	−0.90	0.99	−0.08	0.95	−0.11	0.27	0.11	0.11	Al
			1	−0.02	−0.21	−0.04	0.00	0.14	−0.23	0.05	−0.20	−0.21	−0.31	−0.03	0.00	−0.01	0.03	Fe
				1	+0.20	−0.02	0.07	0.06	−0.07	0.11	−0.05	0.05	−0.02	0.00	−0.00	0.00	0.00	Mn
					1	0.00	0.01	0.05	−0.08	0.25	−0.08	0.49	0.00	0.00	0.00	0.00	0.00	Mg
						1	−0.04	0.00	0.01	0.00	−0.02	0.50	−0.02	0.80	−0.50	0.06	−0.80	Ca
							1	0.37	−0.25	0.23	−0.13	0.00	−0.20	0.06	−0.06	0.00	−0.06	Na
								1	−0.93	0.90	−0.87	0.02	−0.89	0.07	−0.17	−0.07	−0.07	Na+Ti
									1	−0.90	0.92	−0.01	0.89	0.02	0.13	0.16	0.02	Ca+Al
										1	−0.88	0.13	−0.75	0.05	−0.14	−0.07	−0.05	Mg+Ti
											1	−0.10	0.94	−0.10	0.27	0.12	0.10	Na+Al
												1	−0.02	0.44	−0.29	0.03	−0.44	Ca+Mg
													1	−0.11	0.28	0.12	0.11	Al+Mg
														1	−0.67	0.05	1.00	Σ*X*
															1	0.13	0.67	Σ*Y*
																1	−0.05	Σ*Z*(Si)
																	1	19-Σ*X*

B

	Σ*Z*			Σ*Y*			Σ*X*			
	Si	Ti	Al	Fe	Mn	Mg	Ca	Na	Σ*X*	Σ*Y*
Min	17.41	0.07	9.39	1.35	0	0.99	18.37	0.05	18.52	13.28
Max	17.76	1.22	11.11	2.02	0.04	1.44	18.93	0.25	19.03	13.87
Mean	17.58	0.63	10.23	1.54	0.02	1.23	18.60	0.14	18.75	13.67
Std Dev	0.073	0.35	0.50	0.14	0.01	0.11	0.12	0.05	0.12	0.12
Skew	0.18	−0.08	0.16	1.26	−0.22	−0.40	0.67	0.26	0.32	−0.78
Kur	−0.16	−1.16	−1.13	1.90	−0.66	−0.60	0.23	−0.98	−0.29	0.66

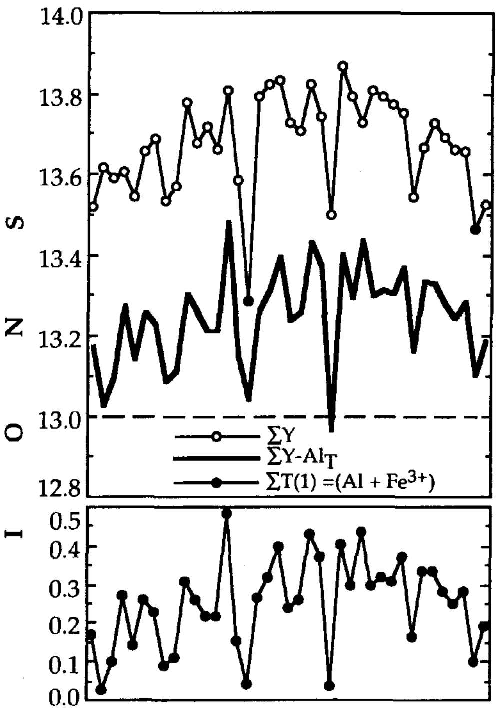

FIG. 3. Plot showing the variation of ΣY, ΣY-Al$_T$ and ΣT1 ions across the 2.5 mm vesuvianite (see text for details).

and

$$^{T(1)}(\mathrm{Al,Fe^{3+}}) + {}^{H(1)}\diamond 2 + {}^{Y}(\mathrm{Mg,Fe^{2+}}) = {}^{T(1)}\diamond + {}^{H(1)}\mathrm{H2} + {}^{Y}(\mathrm{Al,Fe^{3+}})$$

where ◇ denotes a vacancy.

The estimated T(1) cations in the Connemara vesuvianites (see below), correlate negatively with Ca, ^{Y}Al and Mg+Fe^{2+} but also with ^{Z}Al (i.e. Al substituting for Si in the Z sites) confirming the above substitutions but also indicating that $^{T(1)}(\mathrm{Al,Fe^{3+}}) + {}^{Z}\mathrm{Al} = {}^{(H1)}\mathrm{H_2} + {}^{Z}\mathrm{Si}$ is an important form of substitution in the Connemara vesuvianites compared with those published by Groat *et al.* (1994*a*), probably because the Z sites of their published vesuvianites are fully occupied by Si.

The Fe^{2+}/Fe^{3+} ratio is computed in the following way. Iron correlates negatively with Mg and Al (R = −0.21 and −0.18 respectively) indicative of Fe^{2+}>Fe^{3+}. Thus, Fe^{2+}/Fe^{3+} = 0.54 was taken; the assumption is that all Fe^{3+} and Fe^{2+} correlate with Al^{3+} and Mg respectively. The average Connemara vesuvianites have the composition:

$(\mathrm{Ca_{18.60}Na_{0.15}})(\mathrm{Al_{9.81}Ti_{0.63}Fe(III)_{0.71}Fe(II)_{0.83}Mn_{0.02}}$-$\mathrm{Mg_{1.24}})(\mathrm{Al_{0.42}Si_{17.58}})$,

indicating that the T(1) sites are occupied by 0.24 cations. If the Fe^{3+}/Al^{3+} ratios in the Y- and T(1)-sites are the same then the Connemara vesuvianites would have the formula:

$(\mathrm{Ca_{18.60}Na_{0.15}})(\mathrm{Al_{9.59}Ti_{0.63}Fe(III)_{0.69}Fe(II)_{0.83}Mn_{0.02}}$-$\mathrm{Mg_{1.24}})(\mathrm{Al_{0.22}Fe(III)_{0.02}})(\mathrm{Al_{0.42}Si_{17.58}})\mathrm{O_{68}}(\mathrm{OH_{6.36}F_{2.64}O})$.

The SO$_2$ does not exhibit any zoning patterns but correlates negatively with both MgO and TiO$_2$ (R = −0.22) indicative of the substitutions 2H$^+$ + S^{4+} = Mg^{2+} + Ti^{4+} or possibly S^{4+} = Ti^{4+}; S^{4+} = 2Mg^{2+}. The Cl and F substitute for each other; ZnO, which is always between 0.02 and 0.09 wt.%, does not show any preferred core to rim distributions and correlates negatively with Mg suggesting Zn^{2+} = Mg^{2+}.

Phase equilibria and conditions of metamorphism

The internally consistent thermodynamic dataset of Holland and Powell (1990; see also Holland and Powell 1985; Powell and Holland 1985, 1988, 1994)

TABLE 3. Mineral activities and abbreviations used in the text

	Garnet cores					Garnet rim	
	Gr	Alm	Di	Hed	Cats	Gr	Alm
a	0.768	5.3e^{-5}	0.738	0.196	0.0136	0.503	5.86e^{-4}
sd(ln a)	0.0064	0.8337	0.0206	0.1863	0.7353	0.0377	0.7557

The activity of all other minerals is taken as unity except muscovite (a$_{\mathrm{mu}}$ = 0.92).

Mineral abbreviations
Ab = Albite; An = anorthite; Ksp = K-feldspar; Cats = Ca-Tschermak's molecule; Di = Diopside;
Hed = Hedenburgite; Alm = Almandine; Gr = Grossular; Wo = Wollastonite; Cc = Calcite; Qz = Quartz;
Mu = Muscovite; Cor = Corundum; Sill = Sillimanite; And = Andalusite; Ky = Kyanite; Vsv = Vesuvianite;
Zo = Zoisite.

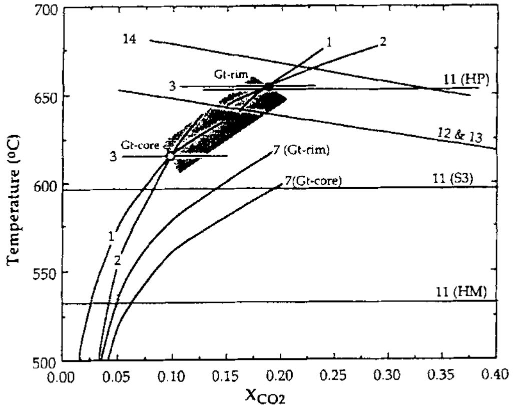

FIG. 4. Isobaric (3.3 kbar) *T-X* plot in the CASCH system for the calc-silicates (the intersections of equilibria 1–3 are shown for $P = 3.3 \pm 0.3$ kbar for garnet core (open circle) and rim (filled circle)). Also shown are reaction 7 for both garnet core and rim and reactions 11–14 in the pelites. HP = Holland and Powell (1990), S3 = prismatic sillimanite of Salje (1986) and HM = Holdaway and Mukhopadhyay (1993). Dark stipple = likely $T\text{-}X_{CO_2}$ in the Omey Granite aureole.

through the program THERMOCALC v1.2 (1990) has been used throughout the study, instead of the elemental partitions between coexisting minerals; the advantages are discussed by Bucker-Nurminen (1990).

The studied sample (BEL 4917) consists of vesuvianite, grossular, diopside, calcite, wollastonite and quartz, defining divariant equilibria in the system CMASCH. As the activity of vesuvianite is unknown (discussed below), the calc silicates phase equilibria will be restricted to the remaining phases taking the mineral activities given in Table 3.

Of the six possible equilibria (Mineral abbreviations are given in Table 3) (1) Cc + Qz = Wo + CO_2; (2) Cats + 2Qz + 2Cc = Gr + $2CO_2$; (3) Cats + Wo = Gr; (4) Alm + 4Qz + 4Cc = 3 Hed + Cats + $4CO_2$; (5) 2Gr + Alm = 3Hed + 3 Cats; and (6) Alm + 6Qz + Cc = Gr + 3Hed + CO_2; only the first three reactions are usable as the a_{alm} is far too low, resulting in large standard errors on activities (Table 3) and hence excluding equilibria 4–6 as potential petrogenetic indicators. Although equilibria 2 and 3 are less useful than reaction 1 due to the large errors in the reactions involving Cats (± 100°C(2σ); T.J.B. Holland, pers. comm.), the first three reactions are considered in the *P-T-X* calculations but with special emphasis on the best experimentally determined reaction 1.

On the $T\text{-}X_{CO_2}$ plot (Fig. 4), the temperature is chosen as <700°C because it is unlikely that contact temperatures exceed 700°C around felsic intrusions such as the Omey Granite. The pressure is restricted to $2<P<4$ kbar because reactions in the pelites (see below) took place within the stability field of andalusite extending to the sillimanite field only in the innermost parts of the aureole. The values of $0.0<X_{CO_2}<0.4$ are taken because the upper limits are defined by the intersections between the pelite and calc-silicate equilibria under the optimum pressure (see below), and bringing in zoisite following the reaction: (7) 3Qz + 5Cc + 2Zo = 3Gr + $5CO_2$ + H_2O, for a_{gr}= 0.768–0.503 indicate $X_{CO_2} \geqslant 0.012$. Similar minimum X_{CO_2} values are obtained using reactions involving Zo-Gr-An.

In the calc-silicates, X_{CO_2} was probably <0.2 because; (a) the occurence of euhedral-subhedral albite, spatially associated with garnet, suggests that Ca in plagioclase was consumed following the reactions; (8) Cc + Wo + (Ca+Na)plag = Gr + CO_2 (+albite); (9) 2Cc + Wo + (Ca+Na)plag = Gr + $2CO_2$ (+albite); (10) 2Wo + (Ca+Na)plag = Gr + Qz (+albite)

Grossular produced through these equilibria is stable only at $X_{CO_2}<0.3$ (Deer *et al.*, 1982), and (b) the coesistence of Mg-vesuvianite, wollastonite and quartz, although the considerable Fe substitution for Mg and F for OH in the present vesuvianites, requires $X_{H_2O}>0.8$ (Valley *et al.*, 1985).

Within the pelites, sillimanite coexists with andalusite in the innermost parts of the aureole and muscovite is broken down to K-feldspar and both andalusite (sillimanite) and corundum suggesting the following CO_2 insensitive equilibria: (11) Sill = And; (12) Qz + Mu = And + Ksp + H_2O; (13) Qz + Mu = sill + Ksp + H_2O; and (14) Mu = Cor + Ksp + H_2O.

When plotted on the $T\text{-}X_{CO_2}$ diagram the curves of reactions 12 and 13, which are believed to be in equilibrium in the present aureole, coincide with each other at $0<X_{CO_2}<0.4$ and $3.6<P<3.0$ kbar for the likely $T = 640 \pm 20$°C (Fig. 4). Under these *P-T* conditions, reaction 14, on the other hand, would only be stable if $0.28<X_{CO_2}<0.60$ for the same temperature range (see below).

The physical conditions of metamorphism around the Omey Granite are best estimated by plotting equilibria 1–3 and 11–13 on a $T\text{-}X_{CO_2}$ plot at $2<P<4$ kbar (Fig. 4). Then, a *P-T* projection of their intersections will trace *P-T* lines, contoured by X_{CO_2}, along which the pelites and calc-silicates could have been in equilibrium. However, since garnet is zoned and despite the uncertainty of the reactions involving Cats, it is more relevant to include the intersections of reactions 1–3 rather than the individual curve of reaction 1 (Fig. 4) so that the isobaric increase of temperature with garnet growth is emphasized especially as X^{gt}_{Mg}increases from core to rim. Figures 4 and 5 indicate that the

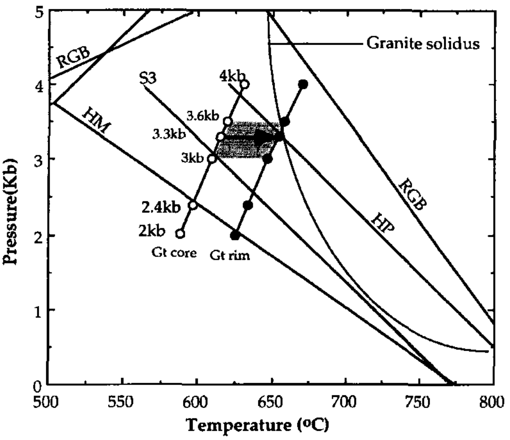

FIG. 5. *P-T* projection diagram showing *P-T* lines along which the pelites and calc-silicates could have been in equilibrium. Dark stipple = likely *P-T* around the Omey Granite. Arrow indicates increasing temperature with garnet growth. RGB = Richardson *et al.* (1969). Other symbols as in Fig. 2.

physical conditions of metamorphism around the Omey Granite were P = 3.3±0.3 kbar, T = 640±20°C, X_{CO_2} = 0.15±0.05. These values are in excellent agreement with those deduced from crystallization of the Omey granite where the Qz-Ab-Or minima follow the X_{H_2O} = 0.8–0.9 curves of Ebadi and Johannes (1991). However, while the values determined above agree with those of Ferguson and Al-Ameen (1985), the pressure is about 0.7 kbar higher. The low-pressure terms obtained by these authors is probably due to the mineral activities of grossular, diopside and muscovite which were not accounted for but also to the fact that their calc-silicate equilibria involve pure anorthite, which is absent from the present calc-silicate and they also used the andalusite-sillimanite equilibrium of Holdaway (1971).

Ferguson and Al-Ameen (1985) argued that the growth of corundum at the expense of muscovite according to reaction 13 above, which occurred about 100 m further away from the granite contact than their Wo + Gr + An assemblage (i.e. 250 m from the granite contact), would require X_{CO_2} of 0.5–0.6. They concluded that H_2O-rich magmatic fluids derived from the main granite body must have percolated through the country rock. Although our results also suggest higher X_{CO_2} ($0.28<X_{CO_2}<0.6$) for this reaction, magmatic fluid was probably insignificant because Ferry (1994) showed that it is very unlikely that such fluids percolate through the country rock for more than 50–100 m for high-level intrusions such as the Omey Granite. Also, it is not at all certain that anorthite exists in the skarn assemblages and its absence invalidates the use of Wo-Gr-An equilibria. Further, there is no convincing evidence that the calc-silicates were in perfect equilibrium with the pelites especially as the CO_2/H_2O ratios could differ even at the same locality depending on the rock composition (e.g. pelites and marbles), porosity, permeability, grain size and diffusivity. The restriction of corundum to within the muscovite plates (Ferguson and Al-Ameen, 1985), suggests that the H_2O released from the decomposing muscovite according to reaction 14 may have locally increased the CO_2/H_2O ratios of the circulating fluids thereby forming corundum at relatively lower temperatures. Some localized convective H_2O-rich fluid might have been involved.

The vesuvianite mole fraction

The *P-T-X* around the Omey Granite are now constrained and hence varying the a_{vsv} for the reaction(s): (15) 2Vsv + 5Wo + CO_2 = 11 Gr + 6Cc Di + $9H_2O$ and/or, (16) 2Vsv + 6Qz = Wo + 11 Gr + 4Di + $9H_2O$, until an agreement with the above-determined *P-T-X* would enable the activity of vesuvianite (a_{vsv}) to be estimated. Taking the relevant mineral activities as given in Table 3, a_{vsv} = 0.01. More importantly, the activity coefficient (γ_{vsv}) could now be computed from the relation $a_{vsv} = X_{vsv}\gamma_{vsv}$ where X_{vsv} = mole fraction assuming an ideal solution.

Based on the formula $Ca_{19}Mg_2Al_{11}Si_{18}O_{69}(OH)_9$, assuming ideal mixing on sites and all the Z, X and Y2 sites are occupied by 18Si, 19Ca and 4Al respectively, Hoisch (1985) proposed the thermodynamic mole fraction:

$$X_{Mg}^{vsv} = 20.4(X_{Mg}^{Y1})(X_{Mg}^{Y3})(X_{Al}^{Y3})^7(X_{OH}^{OH})^7,$$

where $Y1$- and $Y3$-sites refer to B- and AlFe-sites in the terminology of Hoisch (1985). This mole fraction needs to be modified to account for Al for Si and F for OH substitutions and the existence of T1-sites. Thus, the new formula, which is also applicable to B-bearing vesuvianites, becomes:

$$X_{Mg}^{vsv} = 20.4(X_{Ca}^{X})^{19}(X_{Mg}^{Y1})(X_{Mg}^{Y3})(X_{Al}^{Y3})^7(X_{Al}^{T1})^5(X_{Si}^{Z})^{18}(X_{OH}^{OH})^7$$

where:

$(X_{Mg}^{Y1}) = 1 - \mathrm{Fe(II)}^{Y1}$ (if Fe^{2+}/Fe^{3+} ratio is not available then $\mathrm{Fe(II)}^{Y1} = 0.5\ \mathrm{Fe_{tot}}$),

$$(X_{Mg,Al}^{Y3}) = \left(\frac{Mg,Al}{Mg+Al+Ti+Fe^{2+}+Fe^{3+}+Mn^{2+}}\right)^{Y3},$$

$Mg^{Y3} = Mg_{tot} - Mg^{Y1}$; $Al^{Y3} = Al_{tot} - Al^{Y2} - Al^{T}(Al^{Y2} = 4$ a.p.f.u.),

$(X_{\mathrm{Al}}^{T1}) = \left(\frac{\mathrm{Al}}{\mathrm{Al}^{T1}+\mathrm{Fe}^{3+}+\mathrm{B}}\right)$,

$\mathrm{Al}^{T1} + \mathrm{Fe}^{3+} = \Sigma Y$ cations − 13

$(X_{\mathrm{OH}}^{\mathrm{OH}}) = \left(\frac{\mathrm{OH}}{\mathrm{OH+F+Cl+O}}\right)$,

power of seven because 2–3 H^+ ions occur as bonding cations with O(10)s, Groat *et al.*, 1995), $(X_{\mathrm{Ca}}^{\mathrm{X}}), (X_{\mathrm{Si}}^{\mathrm{Z}}) = \left(\frac{\mathrm{Ca}}{\mathrm{Ca+Na}+REE}\right)^{\mathrm{X}}$ and $\left(\frac{\mathrm{Si}}{\mathrm{Si+Al}}\right)^{\mathrm{Z}}$.

If the ΣY cations = 13 and the X and Z sites are fully occupied by Ca and Si respectively and vesuvianite is F- and B-free, then the above formula reduces to Hoisch's(1985).

Using the formula given above, the average Connemara vesuvianites yield $X_{\mathrm{Mg}}^{\mathrm{vsv}} = 0.001$ implying that the $\gamma_{\mathrm{vsv}} = 10$ confirming the non-ideal solution of vesuvianites. The importance of these activity models and the petrogenetic significance of vesuvianite with metamorphic grade will be published elsewhere.

Conclusions

The Connemara vesuvianites have *Y*-cations in excess of 13 a.p.f.u. consistent with an additional tetrahedrally coordinated site (T1) occupied by (Al, Fe^{3+}, B), Groat *et al.* (1994*a*). The zoned vesuvianites show the importance of within-site, mainly among the Y cations, and cross-site, dominated by *X-Y* and *Y-Z* interactions, combined substitutions. The high birefringence zones in vesuvianites are related to high Ti concentrations. The application of a modified thermodynamic mole fraction to the Connemara vesuvianites confirms a non-ideal solution model for the mineral. The studied skarn is consistent with crystallization at 640±20°C at 3.3±0.3 kbar and with $X_{\mathrm{CO_2}}$ at 0.15±0.05 (i.e. $X_{\mathrm{H_2O}} = 0.85\pm0.05$).

Acknowledgements

We thank Mr R. Macdonald and Dr C. Farrow for assistance with the use and calibration of the Cameca SX 50 electron microprobe. Dr T.J.B. Holland is particularly thanked for significant scientific suggestions to improve the first draft.

References

Bucher-Nurminen, K. (1990) Geological phase diagram software. *Terra*, **4**, 401–10.

Deer, W.A., Howie, R.A. and Zussman, J. (1982) *Rock-forming minerals.* volume **1A**, Longman, London.

Ebadi, A. and Johannes, W. (1991) Beginning of melting and composition of first melts in the system Qz-Ab-Or-H_2O-CO_2. *Contrib. Mineral. Petrol.*, **106**, 286–95.

Ferguson, C.C. and Al-Ameen, S.I. (1985) Muscovite breakdown and corundum growth at anomalously low $f_{\mathrm{H_2}}$O: A study of contact metamorphism and convective fluid movement around the Omey Granite, Connemara, Ireland. *Mineral. Mag.*, **49**, 505–14.

Ferguson, C.C. and Harvey, P.K. (1979) Thermally overprinted Dalradian rocks near Cleggan, Connemara, western Ireland. *Proc. Geologists' Assoc.*, **90**, 43–50.

Ferry, J.M. (1994) Role of fluid flow in the contact metamorphism of siliceous dolomitic limestones. *Amer. Mineral.*, **79**, 719–36.

Frimmel, H.E. and van Achterbergh, E. (1995) Metamorphism of calc-silicate and associated rocks in the Pan-African Kaaimans Group, Saldania Belt, South Africa. *Mineral. Petrol.*, **53**, 75–102.

Gibson, R.L. and Wallmach, T. (1995) Complex zoning in vesuvianites from the Canigou Massif, Pyrénées, France. *Canad. Mineral.*, **33**, 77–84.

Groat, L.A., Hawthorne, F.C. and Ercit, T.S. (1992*a*) The chemistry of vesuvianite. *Canad. Mineral.*, **30**, 19–48.

Groat, L.A., Hawthorne, F.C. and Ercit, T.S. (1992*b*) The role of fluorine in vesuvianite: a crystal-structure study. *Canad. Mineral.*, **30**, 1065–75.

Groat, L.A., Hawthorne, F.C. and Ercit, T.S. (1994*a*) Excess Y-group cations in the crystal structure of vesuvianite. *Canad. Mineral.*, **32**, 497–504.

Groat, L.A., Hawthorne, F.C. and Ercit, T.S. (1994*b*) The incorporation of boron into vesuvianite structure. *Canad. Mineral.*, **32**, 505–23.

Groat, L.A., Hawthorne, F.C., Rossman, G.R. and Ercit, T.S. (1995) The infrared spectroscopy of vesuvianite in the OH region. *Canad. Mineral.*, **33**, 609–26.

Hoisch, T.D. (1985) The solid solution chemistry of vesuvianite. *Contrib. Mineral. Petrol.*, **89**, 205–14.

Holdaway, M.J. and Mukhopadhyay (1993) A reevaluation of the stability relations of andalusite: Thermochemical data and phase diagram for aluminium silicates. *Amer. Mineral.*, **78**, 298–315.

Holland, T.J.B. and Powell, R. (1985) An internally consistent thermodynamic dataset with uncertainties and correlations. II Data and results. *J. Meta. Geol.*, **3**, 343–70.

Holland, T.J.B. and Powell, R. (1990) An internally consistent thermodynamic dataset with uncertainties and correlations: The system Na_2O-K_2O-CaO-MgO-MnO-FeO-Fe_2O_3-Al_2O_3-SiO_2-TiO_2-C-H_2-O_2. *J. Meta. Geol.*, **8**, 89–124.

Kerrick, D.M., Crawford, K.E. and Randazzo, A.F. (1973) Metamorphism of calcarous rocks in three roof pendants in the Sierra Nevada, California. *J. Petrol.*, **14**, 303–25.

Leake, B.E. and Tanner, P.W.G. (1994) *The geology of the Dalradian and associated rocks of Connemara, Western Ireland.* Royal Irish Academy, Dublin 96pp.

Leake, B.E., Tanner, P.W.G., and Senior A. (1975) The composition and origin of the Connemara dolomitic marbles and ophicalcites. *J. Petrol.*, **16**, 237–57.

Leggo, P., Compston, W. and Leake, B.E. (1966) The geology of the Connemara granites and its bearing on the antiquity of the Dalradian series. *Q. J. Geol. Soc.*, **122**, 91–116.

Powell, R. and Holland, T.J.B. (1985) An internally consistent thermodynamic dataset with uncertainties and correlations. I Methods and worked example. *J. Meta. Geol.*, **3**, 327–42.

Powell, R. and Holland, T.J.B. (1988) An internally consistent thermodynamic dataset with uncertainties and correlations. III Application methods, worked examples and a computer program. *J. Meta. Geol.*, **6**, 173–204.

Powell, R. and Holland, T.J.B. (1994) Optimal geothermometry and geobarometry. *Amer. Mineral.*, **79**, 120–33.

Richardson, S.W., Gilbert, M.C. and Bell, P.M. (1969) Experimental determination of kyanite-andalusite and andalusite-sillimanite equilibrium; the aluminium silicate triple point. *Amer. J. Sci.*, **267**, 259–72.

Salje, E. (1986) Heat capacities and entropies of andalusite and sillimanite: the influence of fibrolitisation on the phase diagram of the Al_2SiO_5 polymorphs. *Amer. Mineral.*, **71**, 1366–71.

Townend, R. (1966) The geology of some granite plutons from western Connemara, Co, Galway. *Proc. Roy. Ir. Acad.*, **65(B)**, 157–202.

Valley, J.W., Peacor, D.R., Bowman, J.R., Essene, E.J. and Allard, M.J. (1985) Crystal chemistry of Mg-vesuvianite and implications of phase equilibria in the system CaO-MgO-Al_2O_3-SiO_2-H_2O-CO_2. *J. Meta. Geol.*, **13**, 1–12.

[*Manuscript received 28 February 1995: revised 1 November 1995*]